Mapping Landslide Risk of the World

Wentao Yang, Lingling Shen, and Peijun Shi

1 Background

Landslide inventory, susceptibility, and hazard mapping are different steps toward landslide risk mapping (Fell et al. 2008). Landslide inventory can be regarded as a simple form of landslide susceptibility map by showing the location of existing landslides. Besides, other kinds of landslide susceptibility map scan also show the location of potential landslides by incorporating environmental factors, which serve as the basis for hazard and risk mapping (Fell et al. 2008). Although susceptibility map shows the potential location of landslides, it does not give the information of temporal probability. For every location, landslide hazard map shows the spatial and temporal probability of landslides under given intensity (UNESCO 1985), whereas landslide risk map denotes the annual probability of people or economic loss expected. Risk is the interaction of hazard intensity, the vulnerability of elements at risk, and the corresponding environment (Shi 2002).

There are many methods for landslide mapping and landslide disaster, hazard, and risk map are among those popular landslide mappings. Durham Fatal Landslide Database

(Petley 2012) and Landslide Disaster Database from NASA Goddard Space Flight Center (GSFC) (Kirschbaum et al. 2010) are two landslide disaster databases at the global scale. Both databases are collected from worldwide reports of landslide disasters, while the latter has an expansion for other losses except human casualty. Global landslide hazard was mapped by Nadim et al. (2006), who considered global lithology, slope, seismic activity, etc., and assigned hazard probability based on expert judgment. Based on the Gridded Population of the World (GPW), global landslide risk was also estimated in the work carried out by Nadim et al. (2006). Using 3-h resolution TRMM rainfall data, Hong et al. (2006) developed a real-time global landslide warning system based on global landslide susceptibility map. Based on support vector machines (SVM), Farahmand and AghaKouchak (2013) developed a quasi-global landslide susceptibility model using satellite precipitation data, land use and cover change maps, and 250-m resolution topography information.

Previous researches show that slope, altitude, lithology, land use, and soil property can influence landslide susceptibility (Nadim et al. 2006; Cui et al. 2008; Minder et al. 2009; Huang 2011). Coe et al. (2004) and Fabbri et al. (2003) found that slope and altitude are two most important contributing factors of landslide occurrence.

Although Hong et al. (2006) argued that it was possible to map global-scale landslide susceptibility map based on incomplete information layers, the lack of lithology and seismicity layers in this model might impair the hazard map. Compared to the global landslide risk map developed by Nadim et al. (2006), factors including fine temporal resolution rainfall data, tectonic faults, and land use type are considered in this study. By using 15-year consecutive 3-h resolution precipitation data, this study examined every rainfall event over the rainfall threshold for the initiation of landslide. Based on information diffusion theory, information diffusion method was used to fit the 15-year samples to get the expected annual numbers of landslide events.

Mapping Editors: Jing'ai Wang (Key Laboratory of Regional Geography, Beijing Normal University, Beijing 100875, China) and Chunqin Zhang (School of Geography, Beijing Normal University, Beijing 100875, China).
Language Editor: Liu Lianyou (Laboratory of Environmental Change and Natural Disaster, Ministry of Education, Beijing Normal University, Beijing 100875, China).

W. Yang · L. Shen
Academy of Disaster Reduction and Emergency Management, Ministry of Civil Affairs and Ministry of Education, Beijing Normal University, Beijing 100875, China

P. Shi (✉)
State Key Laboratory of Earth Surface Processes and Resource Ecology, Beijing Normal University, Beijing 100875, China
e-mail: spj@bnu.edu.cn

By combining these results, landslide hazard map with the LandScan population and global landslide disaster database (Kirschbaum et al. 2010), population vulnerability and mortality risk of landslide of the world were calculated. In this study, the environmental factors denote the background of hazard formation, while the probability of hazard is estimated from precipitation data. At global scale, vulnerability of human is estimated from the ratio of casualties to exposed population at national level.

2   Method

Figure 1 shows the technical flow chart for mapping landslide risk of the world.

2.1   Hazard

This study can be divided into three components: landslide susceptibility, hazard, and mortality risk mapping. By weighting layers such as slope, elevation, land use type, lithology, fault, and semi-quantitative seismic hazard map, landslide susceptibility map was developed. TRMM 3B42 3-h precipitation data (Appendix III, Hazards data 4.4) were used to generate hazard map by integrating previously developed landslide susceptibility map. Finally, LandScan population data (Appendix III, Exposures data 3.1) and global landslide casualty data (Appendix III, Disasters data 5.2) were used to calculate population vulnerabilities of each country and landslide risk to population. Due to limited data at the global scale, the global hazard mapping was validated by the global landslide hotspot hazard map.

2.1.1   Global Landslide Susceptibility

Landslide susceptibility map was calculated by weighting different layers of preparatory or environmental layers, including slope, elevation, lithology, active fault line density, and seismicity (Eq. 1). The weight of each layer is given according to their importance to landslides referring to past research (Nadim et al. 2006; Hong et al. 2007).

$$\text{Sus} = 0.25 \times \text{Slo} + 0.15 \times \text{DEM} + 0.15 \times \text{LUCC} + 0.15 \\ \times \text{Lith} + 0.15 \times \text{Fault} + 0.15 \times \text{Seis}$$

$$(1)$$

where Sus denotes landslide susceptibility, Slo denotes reclassed global slope percentage (Appendix III, Environments data 2.2), DEM denotes normalized global elevation (Appendix III, Environments data 2.1), LUCC denotes reclassed global land use data in 2012 (Appendix III, Environments data 2.8), Lith denotes reclassed global lithology data (Appendix III, Environments data 2.4), Fault denotes reclassed global active fault line density (Appendix III, Environments data 2.4), and Seis denotes seismicity (PGA) (Appendix III, Hazards data 4.1).

2.1.2   Global Landslide Hazard

By considering the temporal occurrence of landslide triggers such as precipitation, landslide hazard map can be made based on susceptibility map (van Westen et al. 2008). Fine-temporal resolution precipitation data are vital for estimating the occurrence of rainfall-induced landslides. However, rain gauge stations are unevenly distributed and cover very limited areas around the world. Thus, the homogeneous global coverage TRMM data are ideal for calculating the occurrence of landslides.

Fig. 1 Technical flowchart for mapping landslide risk of the world
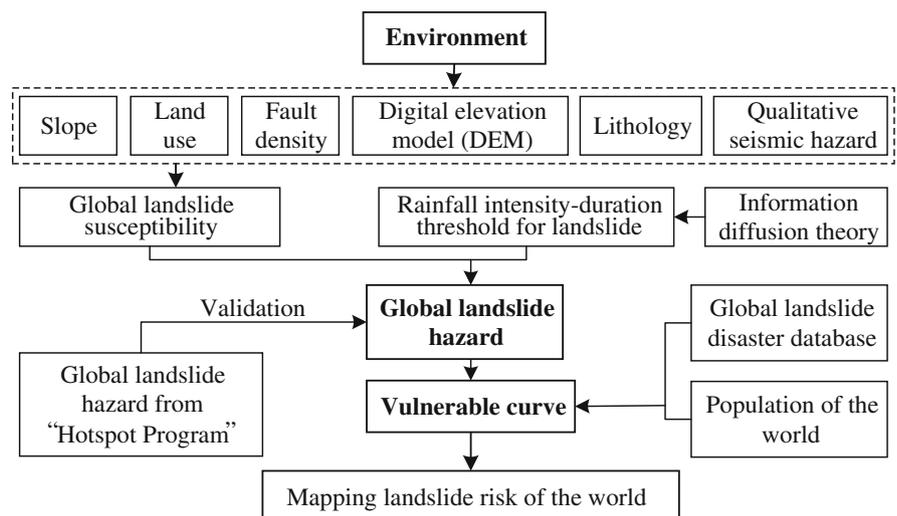
The data used were TRMM 3B42. However, there are some deviations between station-based precipitation and TRMM-based data (Qi et al. 2013). Most existing station-based precipitation threshold are not necessarily sufficient for landslide hazard analysis. Based on global landslide records and TRMM data, Hong et al. (2006) established a global rainfall threshold for the initiation of landslides. This study used Hong's threshold to examine every rainfall event in each pixel from the beginning of 1998 to the end of 2012 (Eq. 2).

$$I = 12.45D^{-0.42} \qquad (2)$$

where I is the precipitation intensity (mm/h) and D is the rainfall duration (h).

After examining every rainfall event, we summed up the number of events that exceed the threshold each year for each pixel. So, there are 15 years data with the number of landslide events from 1998 to 2012.

For the hazard factors with limited samples, it is a better choice to apply information diffusion theory (Huang and Moraga 2004). The normal diffusion model was the most frequently used kind of information diffusion model. The process of information diffusion was actually to diffuse the information in single sample to the whole sample space, which obeys the principle of conservation of the amount of information.

The data scope of TRMM was among 50° latitude north and south. For areas beyond this scope, the NCEP/NCAR reanalysis data (Appendix III, Hazards data 4.5) were used. The high-latitude areas had less landslide occurrences due to relatively high vegetation cover, soil freezing, sparsely populated, and subdued topography. Applying the methods and processes mentioned above, with the same period as TRMM (January 1, 1998—December 31, 2012), the cumulative value of global precipitation–landslide exceedance threshold was calculated.

After getting global precipitation–landslide frequency, according to the different weights of susceptibility map, the global landslide hazard map can be estimated (Eq. 3):

$$H(\text{pre}) = \text{Sus} \times \text{Pre} \qquad (3)$$

where $H(\text{pre})$ is the number of rainfall-induced landslides (times/a/km^2), Sus is the landslide susceptibility, and Pre is the annual expectation numbers of exceedance precipitation–landslide threshold (times/a/km^2).

2.2 Mortality Risk

Vulnerability typified the loss and damage of exposure by hazard. Generally, the loss was estimated from statistical history loss data. Population vulnerability of landslide is estimated by the statistical casualties and population exposure. NASA's global landslide early warning system based on TRMM data had collected the data of human death and missing due to precipitation-induced landslide in 2003 and 2007–2011 (Appendix III, Disasters data 5.2). According to corresponding year, the exposed population of each country and region was calculated in the light of LandScan 2010 and the hazard in the same site; the landslide–casualties vulnerability curve was made by combing casualties (Fig. 2).

There were 76 countries with available statistical mortality data in 2003 and 2007–2011(Kirschbaum et al. 2010). To supplement the inadequate data, similar vulnerability value was assigned to countries with geographical proximity.

On the basis of global landslide hazard raster map (0.25° × 0.25°) and global landslide–casualties vulnerability, adding the layer of global population density raster map
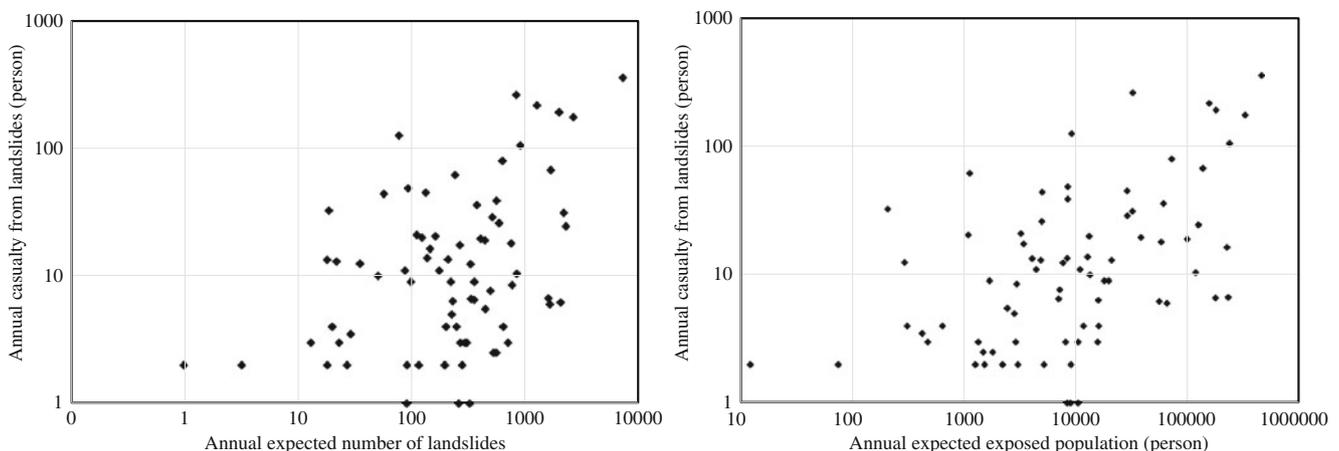

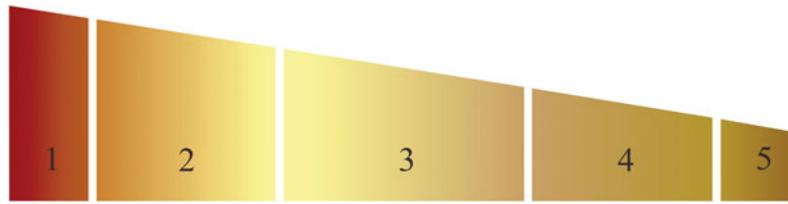**Fig. 2** Landslide–casualties vulnerability curve

Fig. 3 Expected annual mortality risk levels of landslide of the world *1* (0, 10 %] China, Brazil, Iran, Uganda, Philippines, Indonesia, India, Nepal, Paraguay, Bolivia, Burundi, Colombia. *2* (10, 35 %] Switzerland, Pakistan, Bangladesh, Afghanistan, Guatemala, Portugal, South Korea, Peru, Sierra Leone, Cameroon, Vietnam, Central African Republic, Guinea-Bissau, Kazakhstan, Congo (Democratic Republic of the), Mexico, Angola, Nigeria, Syria, Dominican Republic, Ethiopia, Tajikistan, Costa Rica, Sri Lanka, Jordan, Malaysia, El Salvador, North Korea, Haiti, Tanzania, Senegal, *3* (35, 65 %] Spain, Guinea, Iraq, Kyrgyzstan, Mali, Liberia, Uzbekistan, Thailand, Mozambique, Kenya, Rwanda, Romania, Madagascar, Malawi, Italy, Sudan, Ecuador, Zambia, Papua New Guinea, Yemen, Japan, Uruguay, France, Turkey, Zimbabwe, Georgia, Venezuela, United States, Azerbaijan, Panama, South Africa, Honduras, Poland, Niger, Laos, Chile, Cuba, New Zealand. *4* (65, 90 %] Ghana, Burkina Faso, Algeria, Slovakia, Russia, Nicaragua, Argentina, Armenia, Morocco, Serbia, Jamaica, Bhutan, Palestine, Bosnia and Herzegovina, Trinidad and Tobago, Bulgaria, Moldova, Ukraine, Australia, Tunisia, Israel, Mauritania, Chad, Germany, Togo, Hungary, Lebanon, Austria, Greece, Croatia, Albania *5* (90, 100 %] Macedonia, Saudi Arabia, Somalia, Eritrea, Lesotho, Slovenia, Czech Republic, Montenegro, Cambodia, Turkmenistan, Mongolia, Libya

(1 km × 1 km) from American LandScan program, world mortality risk of landslide was obtained (Eq. 4).

$$R_{pop} = V \times H \times E_{pop} \tag{4}$$

where R_{pop} is landslide-induced mortality risk, V is the population vulnerability, H is landslide hazard, and E_{pop} is global population density.

3 Results

Susceptibility represents the likelihood of landslide occurrence, that is, how easily landslide could occur under a certain environment. From the aspect of disaster system theory, susceptibility is subjected to the instability of landslide hazard-background environment. Global landslide susceptibility is divided into 5 classes, from high to low, expressing a stable progressive decrease. The highest class is distributed mainly around the major structural mountains, especially in the Alpine–Himalayan mountain tectonic belt, the Pacific Rim, and the Great Rift Valley. The medium and lower classes are scattered in plateaus, such as African plateau, Chinese Loess plateau, Yunnan–Guizhou plateau, Inner Mongolian plateau, India's Deccan plateau, and the edge of Brazil plateau.

Rainfall-induced landslide hazard indicates the estimation of landslide numbers in different susceptibility classes under different precipitation intensities. Global rainfall-induced landslides are mainly scattered in humid areas with large undulating terrain, such as windward slope of the southern Himalayas, China Longmen Mountain area Mt. Alps, and the Andes.

Global landslide mortality risk mainly distributes in mountain areas with high population density, especially in the developing countries. Countries with high landslide mortality risk include China (southwestern area), India (northern part, southern Himalayas), Nepal, Pakistan (northern area), Italy, and countries in Central and South America.

By zonal statistics of the expected risk result, the expected annual mortality risk of landslide of the world at national level is derived and ranked (Fig. 3). The top 1 % country with the highest mortality risk of landslide is China, and the top 10 % countries are China, Brazil, Iran, Uganda, Philippines, Indonesia, India, Nepal, Paraguay, Bolivia, Burundi, and Colombia.
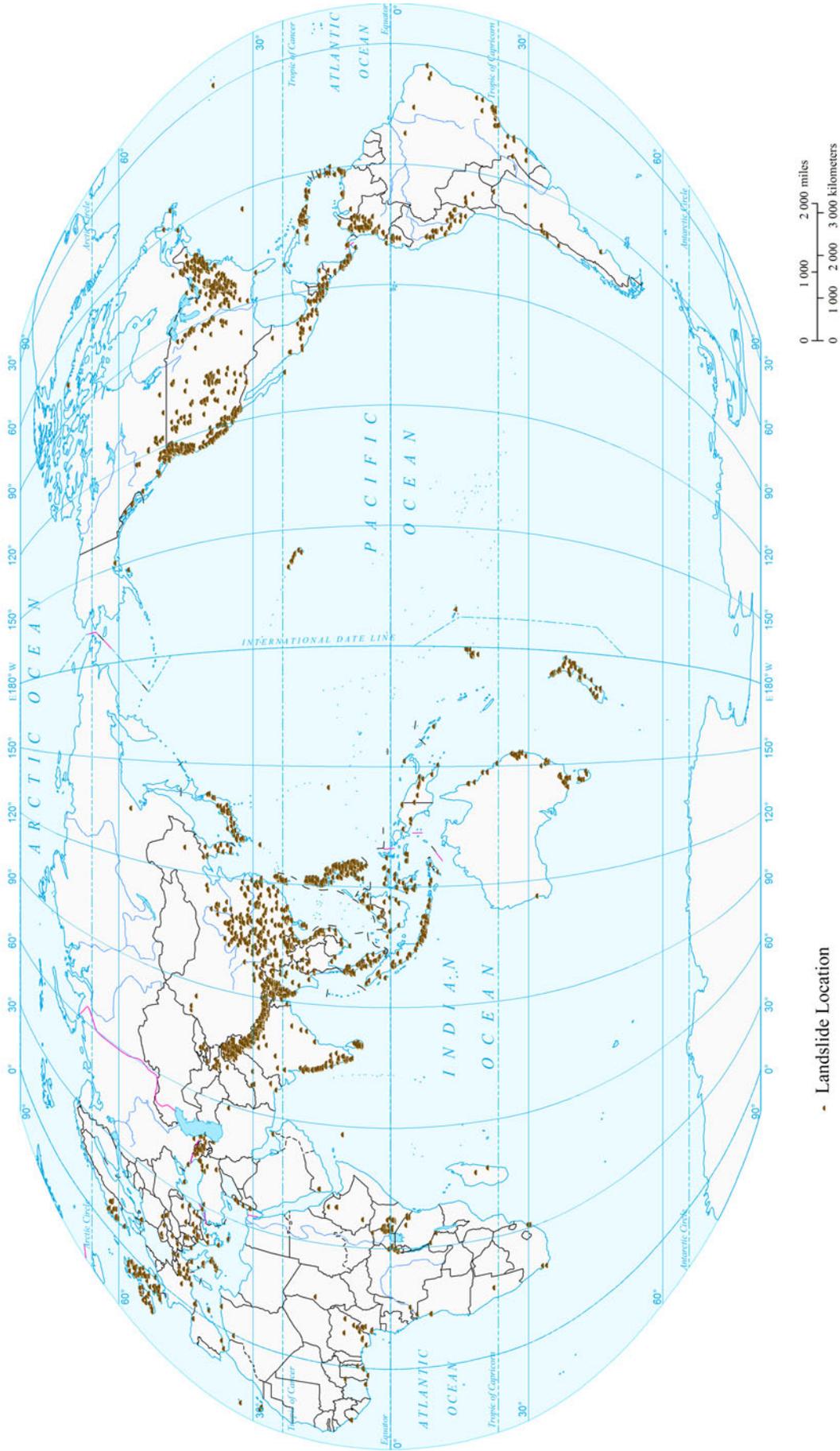
4 Maps

Earthquake, Volcano and Landslide Disasters

Landslide

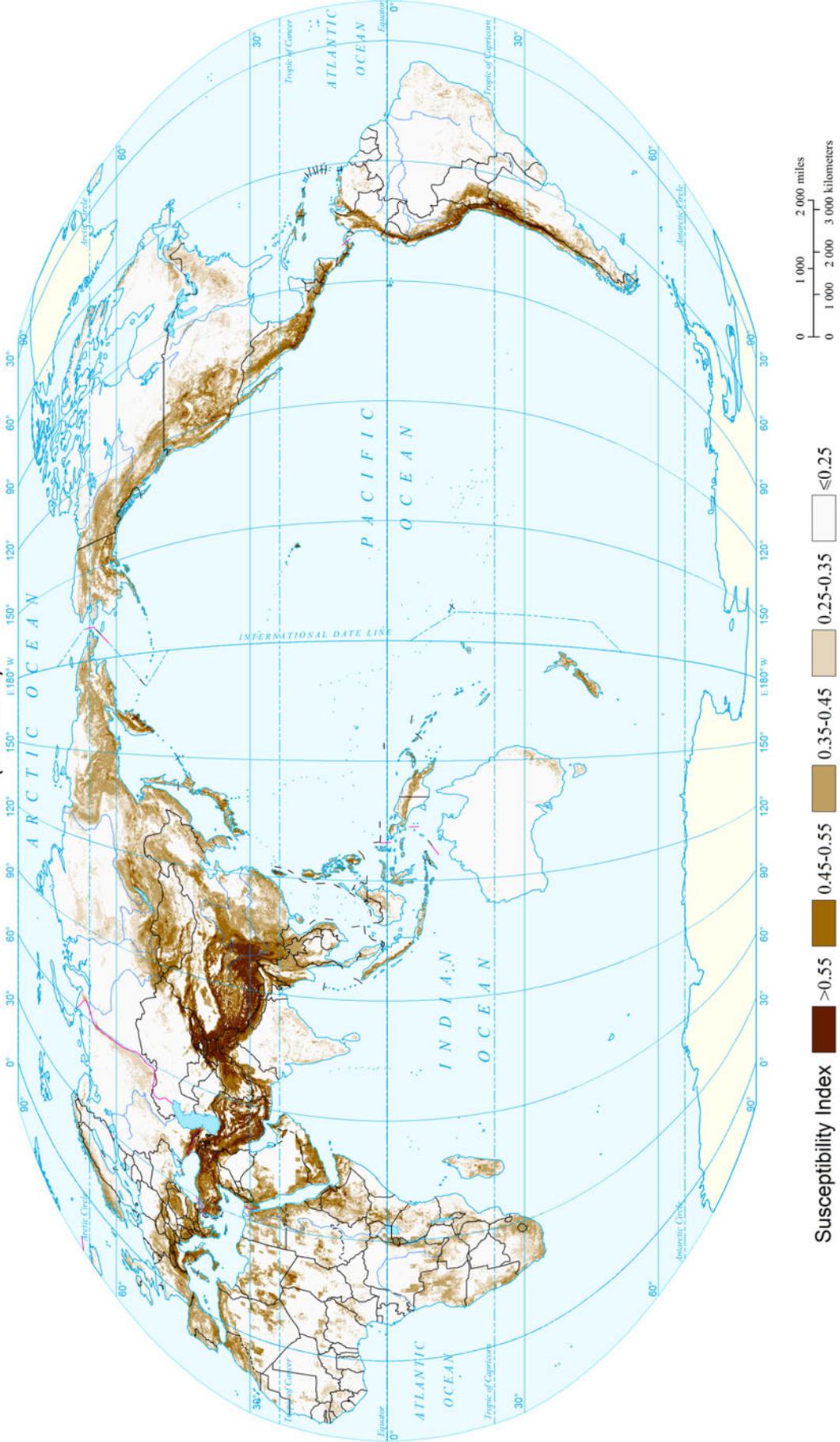Historical Event Locations of Global Landslide (2003 and 2007-2011)

- Landslide Location

Data Source: National Aeronautics and Space Administration(NASA)
http://gcmd.nasa.gov/records/GCMD_NASA_GSFC_TRMM_LANDSLIDE_INVENTORY.html

Earthquake, Volcano and Landslide Disasters

Landslide

Global Landslide Susceptibility
(0.1°×0.1°)

Susceptibility Index

>0.55	0.45-0.55	0.35-0.45	0.25-0.35	≤0.25

Earthquake, Volcano and Landslide Disasters

Landslide

Global Rainfall-induced Landslide Intensity
(0.25°×0.25°)

Intensity Index
- >3
- 1-3
- 0.5-1
- 0.1-0.5
- ≤0.1

Landslide

Earthquake, Volcano and Landslide Disasters
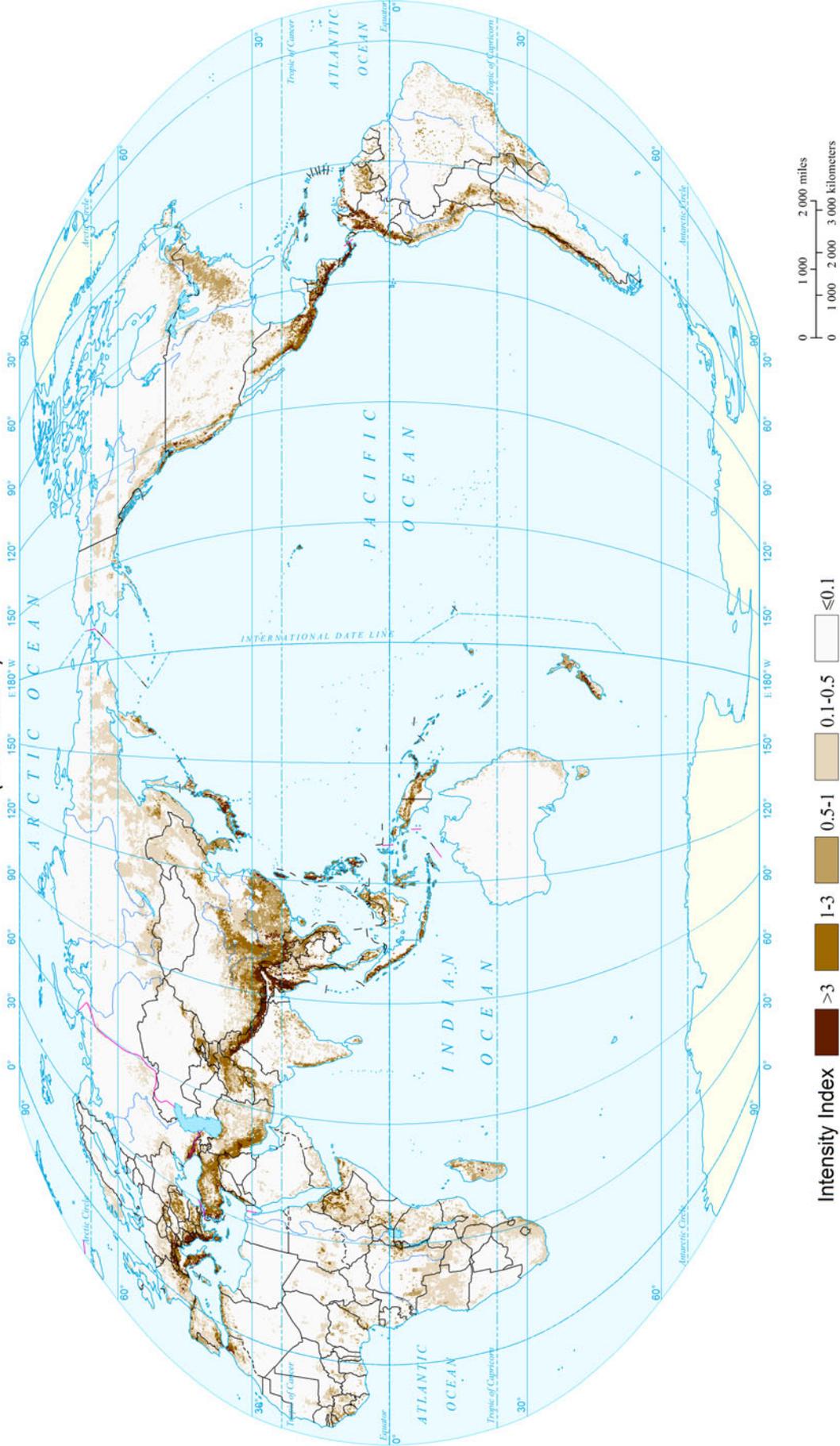
Expected Annual Mortality Risk of Landslide of the World
(0.25°×0.25°)

Mortality (person)

| >0.1 | 0.05-0.1 | 0.005-0.05 | 0.001-0.005 | ≤0.001 |
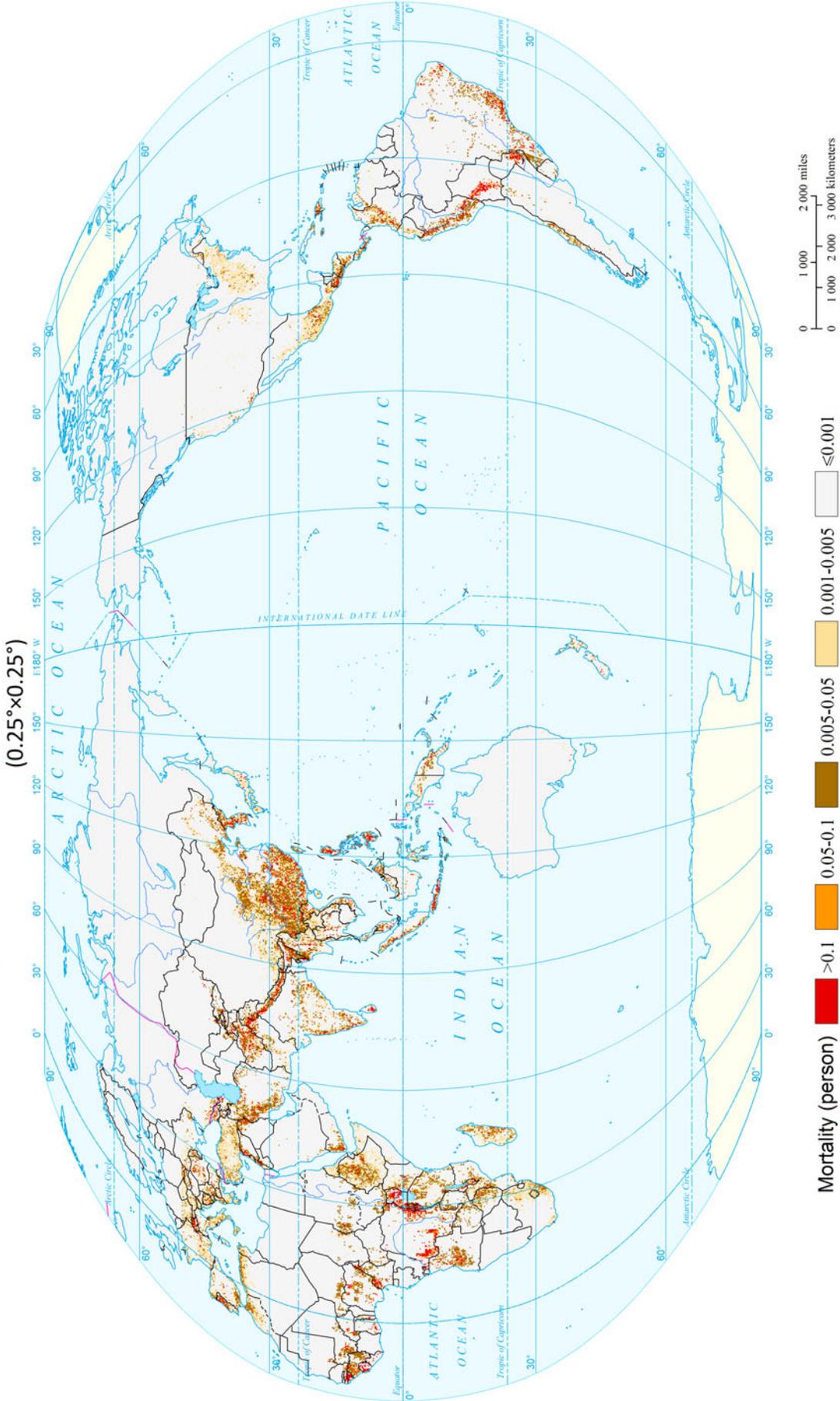
Expected Annual Mortality Risk of Landslide of the World
(Comparable-geographic Unit)

Mortality (person) ■ >75 ■ 35-75 ■ 15-35 □ 1-15 □ ≤1

0 1 000 2 000 miles
0 1 000 2 000 kilometers
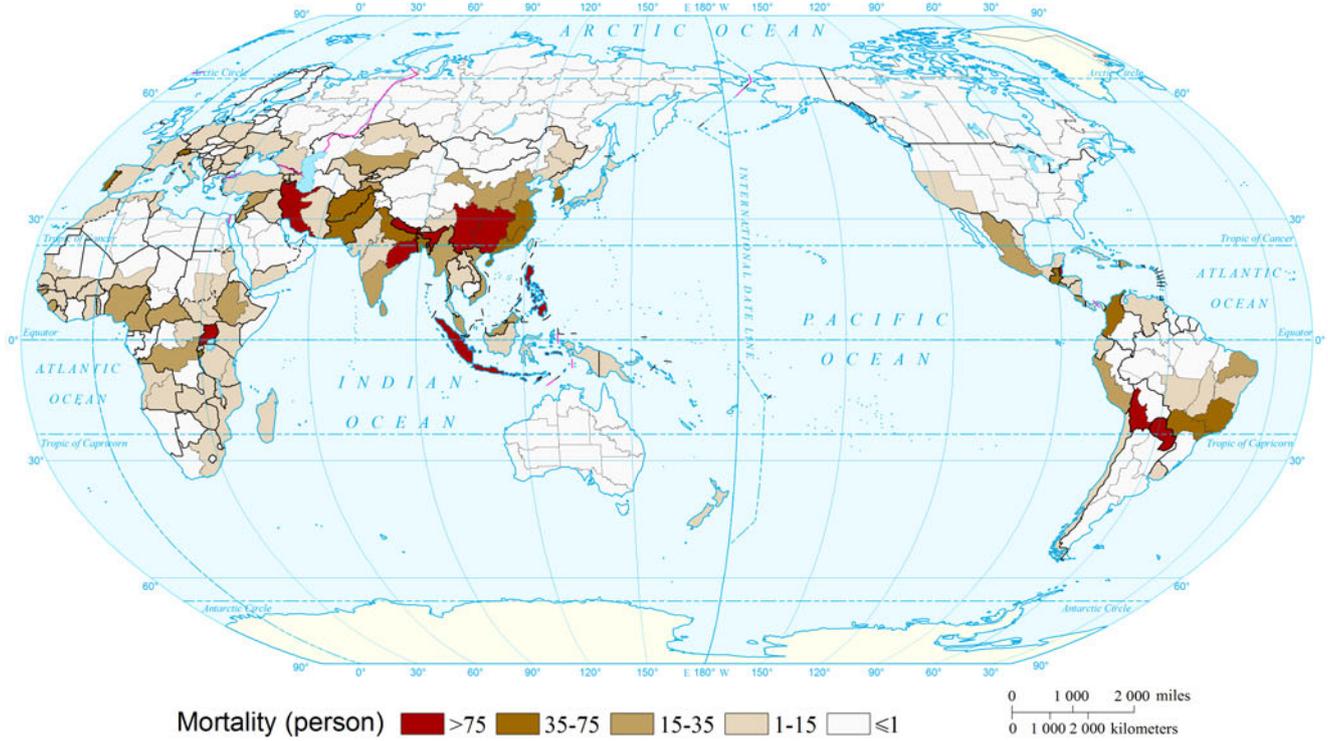
Expected Annual Mortality Risk of Landslide of the World
(Country and Region Unit)

Mortality ■ >200 ■ 50-200 ■ 10-50 □ 1-10 □ ≤1

0 1 000 2 000 miles
0 1 000 2 000 kilometers
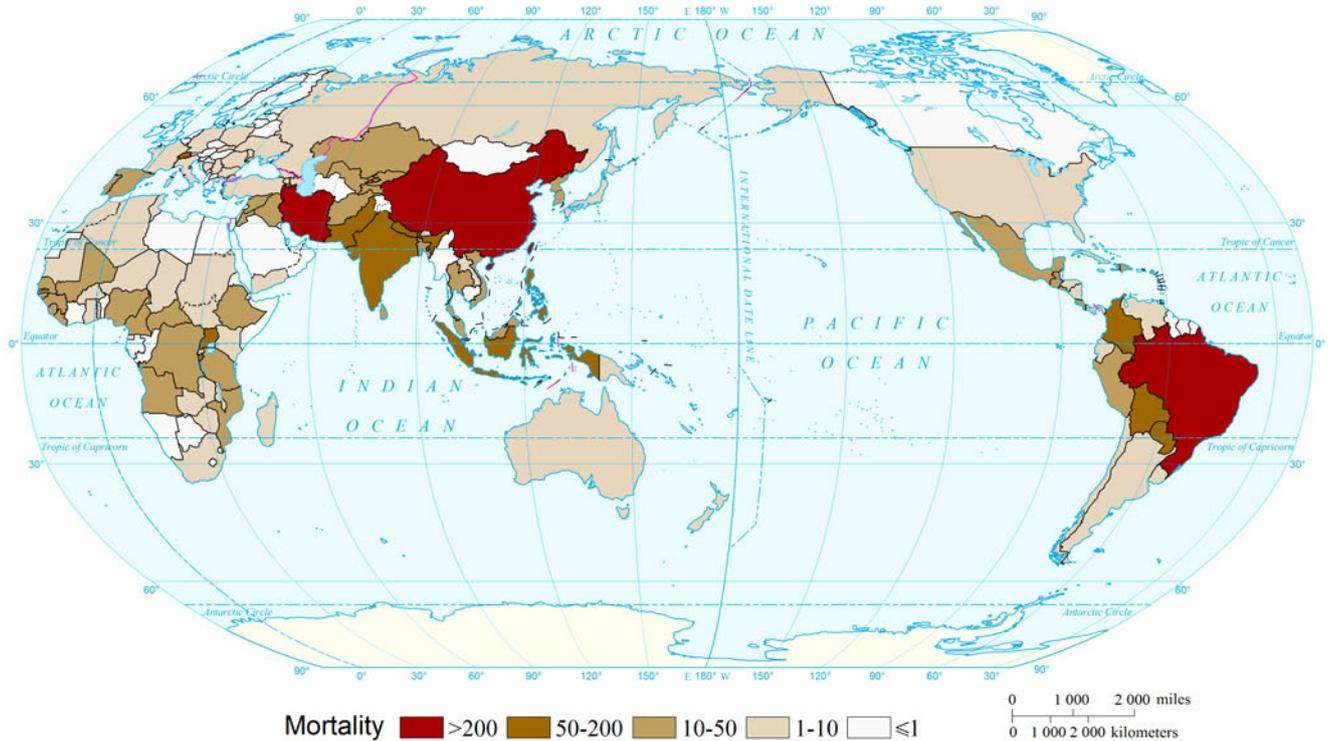
References

Coe, J.A., J.W. Godt, R.L. Baum, et al. 2004. Landslide susceptibility from topography in Guatemala. In *Landslides: Evaluation and stabilization*, vol. 1, ed. W.A. Lacerda, M. Ehrlich, and S.A.B. Fontura, et al. 69–78. London: Taylor & Francis Group.

Cui, P., F.Q. Wei, S.M. He, et al. 2008. Mountain disasters induced by the earthquake of May 12 in Wenchuan and the disasters mitigation. *Journal of Mountain Science* 26(3): 280–282. (in Chinese).

Fabbri, A.G., C.J.F. Chung, A. Cendrero, et al. 2003. Is prediction of future landslides possible with a GIS? *Natural Hazards* 30(3): 487–503.

Farahmand, A., and A. AghaKouchak. 2013. A satellite-based global landslide model. *Natural Hazards and Earth System Science* 13(5): 1259–1267.

Fell, R., J. Corominas, C. Bonnard, et al. 2008. Guidelines for landslide susceptibility, hazard and risk zoning for land use planning. *Engineering Geology* 102(3–4): 99–111.

Hong, Y., R. Adler, and G. Huffman. 2006. Evaluation of the potential of NASA multi-satellite precipitation analysis in global landslide hazard assessment. *Geophysical Research Letters* 33(22). doi:10. 1029/2006GL028010.

Hong, Y., R. Adlerand, and G. Huffman. 2007. Use of satellite remote sensing data in the mapping of global landslide susceptibility. *Natural Hazards* 43(2): 245–256.

Huang, C.F., and C. Moraga C. 2004. A diffusion-neural-network for learning from small samples. *International Journal of Approximate Reasoning* 35: 137–161.

Huang, R.Q. 2011. After effect of geohazards induced by the Wenchuan earthquake. *Journal of Engineering Geology* 19(2): 145–161. (in Chinese).

Kirschbaum, D.B., R. Adler, Y. Hong, et al. 2010. A global landslide catalog for hazard applications: Method, results, and limitations. *Natural Hazards* 52(3): 561–575.

Minder, J.R., G.H. Roeand, and D.R. Montgomery. 2009. Spatial patterns of rainfall and shallow landslide susceptibility. *Water Resources Research* 45(4). doi:10.1029/2008WR007027.

Nadim, F., O. Kjekstad, P. Peduzzi, et al. 2006. Global landslide and avalanche hotspots. *Landslides* 3(6): 159–173.

Petley, D. 2012. Global patterns of loss of life from landslides. *Geology* 40(10): 927–930.

Qi, W.W., B.P. Zhang, Y. Pang, et al. 2013. TRMM-data-based spatial and seasonal patterns of precipitation in the Qinghai-Tibet Plateau. *Scientia Geographica Sinica* 33(8): 999–1005. (in Chinese).

Shi, P.J. 2002. Theory on disaster science and disaster dynamics. *Journal of Natural Disasters* 11(3): 1–9. (in Chinese).

United Nations Educational, Scientific and Cultural Organization (UNESCO). 1985. *Landslide hazard zonation: A review of principles and practice*. Paris: United Nations Educational Scientific and Cultural Organization.

van Westen, C.J., E. Castellanos, and S.L. Kuriakose. 2008. Spatial data for landslide susceptibility, hazard, and vulnerability assessment: An overview. *Engineering Geology* 102(3): 112–131.